Available online at www.sciencedirect.com
ScienceDirect
Polymer 48 (2007) 1012–1019
polymer
www.elsevier.com/locate/polymer

Mobile amorphous phase fragility in semi-crystalline polymers: Comparison of PET and PLLA

M. Arnoult [a], E. Dargent [a,*], J.F. Mano [b,c]

[a] Laboratoire PBM, UMR 6522, LECAP, Institut des Matériaux de Rouen, Université de Rouen, Faculté des Sciences, Avenue de l'Université BP 12, 76801 Saint Etienne du Rouvray, France
[b] 3B's Research Group: Biomaterials, Biodegradables and Biomimetics, University of Minho, Campus de Gualtar, 4710-057 Braga, Portugal
[c] Polymer Engineering Department, University of Minho, Campus de Azurém, 4800-058 Guimarães, Portugal

Received 23 October 2006; received in revised form 21 December 2006; accepted 31 December 2006
Available online 22 January 2007

Abstract

PET and PLLA were cold crystallised at various times and the two polymers were studied by differential scanning calorimetry (DSC), dielectric spectroscopy (DS) and thermally stimulated depolarisation currents (TSDC). The crystalline, the amorphous and the rigid amorphous fraction were quantified. The percentage of rigid amorphous fraction is very large in semi-crystalline PET and very low in semi-crystalline PLLA. From DSC, DS and TSDC data, the values of the relaxation times of four samples were obtained above and below the glass transition. The ''strong-fragile'' glass former liquid concept was used and the fragility of polymers was obtained. The presence of the crystalline phase and of a rigid amorphous fraction does not significantly modify PLLA fragility parameters and the polymer remains ''fragile'', while for PET the semi-crystalline material goes towards a ''strong character''. The coupling between phases is much weaker in PLLA than in PET.

Keywords: PET; PLLA; TSDC

1. Introduction

Poly(ethylene terephthalate) PET is one of the most widely used polymers in the domain of packaging applications due to its excellent combination of properties such as good mechanical properties, transparency, and easy processing. Its reasonably high gas barrier properties allow to understand why PET became the first choice as a material for soft drink bottles. Polymers like poly(L-lactic acid) (PLLA) have received a greater attention as an alternative polymer for packaging. Indeed, PLLA is a biodegradable thermoplastic, produced from annually renewable resources. It shows mechanical and barrier properties comparable to PET [1]. These two semi-crystalline polyesters can be quenched from the melt to the amorphous glass and cold crystallisation leads to various degrees of crystallinity. The semi-crystalline polymers consist of a crystalline phase, an amorphous phase and tie molecules appearing in both phases. Because of the usual incomplete decoupling (due to geometrical constraints), a part of the amorphous phase could appear with different properties. For 20 years, a three-phase model has been proposed and the affected part of the amorphous phase was called rigid amorphous fraction RAF [2,3]. This fraction can be easily characterised by thermal analysis [4] because it does not participate in the glass transition of the amorphous phase (called mobile amorphous phase MAP). Wunderlich has shown the RAF may not remain rigid up to the melting temperature but seems to decrease and disappear gradually above the glass transition temperature T_g of the MAP [5]. In a recent work, Androsch [6] has shown, in various annealed PET, that the amount of RAF must be considered as a measure of the coupling between the crystalline and the amorphous phase. In this work, we propose to investigate the coupling between the RAF and the mobile amorphous

* Corresponding author. Tel.: +33 2 32 95 50 83; fax: +33 2 32 95 50 82.
E-mail address: eric.dargent@univ-rouen.fr (E. Dargent).

0032-3861/$ - see front matter © 2007 Elsevier Ltd. All rights reserved.
doi:10.1016/j.polymer.2006.12.053

phase. First, the evolution of the coupling between the crystalline and the amorphous phases in PLLA and PET was compared for various percentages of crystalline phase. Then, by comparing the response of the remaining amorphous phase of PLLA and PET, we have studied how the intrinsic parameters of the MAP are modified by the presence of the RAF and the crystalline phase. The mobile amorphous phase was studied using the ''strong-fragile'' glass former liquid concept proposed by Angell [7] and the variation of the characteristic relaxation time was analysed for temperatures below and above the glass transition. The ''fragility concept'' allows the definition of a fragility index m [8] which is a measure of the way the relaxation time τ (or related properties) decreases with increasing temperature around T_g. A low value m (≈ 16) characterises a ''strong'' glass-forming liquid, exhibiting an Arrhenian temperature dependence of τ as observed, for example, for rigid network systems [9], while a ''fragile'' glass-forming liquid with a high m value (≈ 200) exhibits an important sensitivity of its properties with the temperature. In this case, this dependence observed, for example, for linear polymeric materials [10,11] could be fitted by a Vogel–Tamman–Fulsher relationship [12–14]. The structural relaxation and the fragility of PET have often been studied [15–21]. For instance, it has been shown that the MAP of a PET film varies with a uniaxial drawing: for undrawn or weak draw ratio, the PET is amorphous and can be classified as ''fragile'' ($m = 142$), while for high draw ratio the PET is semi-crystalline and classified as ''strong'' ($m = 66$) [22]. The glass transition and the fragility of PLLA have not been thoroughly studied. Recently, the glass transition dynamics of both amorphous and semi-crystalline PLLA were investigated by differential scanning calorimetry (DSC) [23]; in this case no significant variation of the fragility index was observed and the PLLA amorphous phase seems to remain ''fragile'' with $m \approx 150$. In order to characterise the materials above and below the glass transition temperature, our following work was based on three complementary techniques: DSC, dielectric spectroscopy (DS) and thermally stimulated depolarisation currents (TSDC). Moreover, the different chemical structures of these two polyesters (Fig. 1) led, upon crystallisation, to different morphologies at the lamellar level. This allowed to find more reliable structure/morphology/glass transition dynamics relationships and helped to generalise the conclusions obtained.

2. Experimental

Initial poly(ethylene terephthalate) (PET) material is obtained from a 500 μm thick film extruded by Carolex Co. The number-average molecular weight is $\overline{M}_n = 31,000$ g mol^{-1} and the weight-average molecular weight is $\overline{M}_w = 62,000$ g mol^{-1}. The film is isotropic and practically amorphous judging from birefringence, density and X-ray diffraction measurements. Samples of poly(L-lactic acid) (PLLA) are from Cargill Dow. The poly(L-lactic acid) (PLLA) used in this work is of high stereoregularity. The specific optical rotation $[\alpha]_D^{25}$ of this PLLA is 154.7 as measured in chloroform at a concentration of 1 g/dl and 25 °C (AA-1000 polarimeter). PLLA was estimated to have a L-lactide content of 99.6% by assuming $[\alpha]_D^{25}$ of poly(L-lactic acid) and poly(D-lactic acid) to be −156 and 156, respectively [24]. About 300 μm thick PLLA films were obtained by pressing at 185 °C for 2 min under 200 bar followed by a quench in cold water. Number-average molecular weight is $\overline{M}_n = 69,000$ g mol^{-1} and polydispersity is 1.73. Semi-crystalline samples are obtained by the following in situ procedure in the DSC apparatus: first, a sample of 10 ± 1 mg was heated above the fusion temperature for 2 min (300 °C and 180 °C for PET and PLLA, respectively) and cooled as fast as possible (≈ 50 °C/min) to obtain an as amorphous as possible sample. Then, the sample was cold crystallised at a temperature T_a above the glass transition temperature ($T_a = 100$ °C and 80 °C for PET and PLLA, respectively) for time t_a included between 0 and 720 min. Finally, the sample was cooled down to 30 °C and heated up at 10 °C/min in order to obtain the DSC curves. This thermal cycle was repeated on the same samples to obtain the different DSC curves. For TSDC and DS analysis, the initial amorphous films were directly analysed and semi-crystalline materials were obtained after crystallisation in ovens at the same T_a temperatures as for the DSC analysis. The DSC apparatus from Thermal Analysis Instrument is a Q100 calibrated in temperature and energy (at 10 K/min under nitrogen atmosphere) using indium and zinc standards. The DSC curves presented in this paper have been normalised to 1 mg of matter. The given T_g temperatures are mid-point temperatures. Dielectric measurements were performed by means of a dielectric analyser (Thermal Analysis Instrument DEA 2970), with a frequency range between 0.01 Hz and 300 kHz, from 40 °C to 150 °C by the steps of 5 °C. The studied samples were 25 mm in diameter and 0.5 mm thick disks for PET and PLLA. For each measuring point, the real and the imaginary part of the dielectric permittivity as well as the temperature and the frequency were recorded. TSDC measurements described in detail elsewhere [25] were performed, thanks to an apparatus developed in our laboratory [26]. At a polarisation temperature T_p just above the glass transition (typically $T_p = T_g$ endset), samples were subjected to an electric field ($E = 10^6$ V/m) for 2 min. Then, the temperature was lowered to −10 °C, samples were

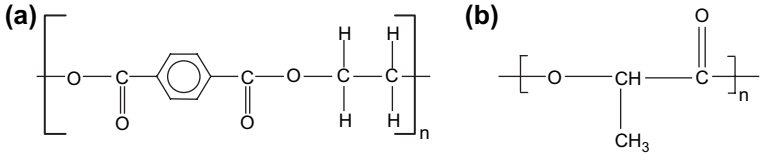

Fig. 1. PET and PLLA constitutive units (a. PET; b. PLLA).

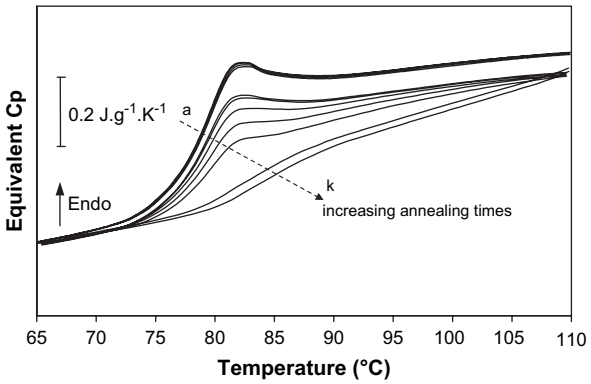

Fig. 2. DSC curves around the glass transition of a PET cold-crystallised at 100 °C for different times (from a to k: 2, 20, 40, 60, 90, 120, 180, 240, 300, 420 and 720 min). Equivalent Cp is the heat flow normalised to the mass and to the heating ramp.

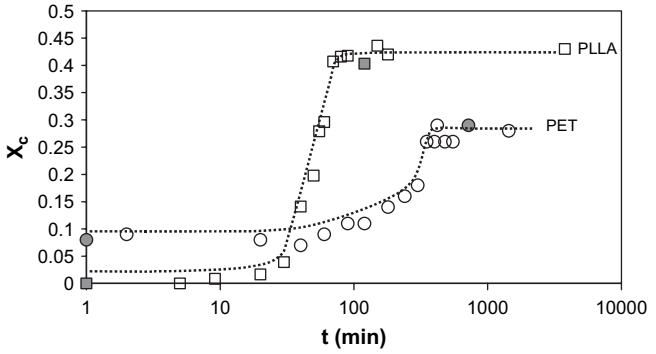

Fig. 4. Degree of crystallinity variations as a function of the annealing time at 100 °C and 80 °C for PET (circles) and PLLA (squares), respectively. The grey points represent samples focused on in this paper.

short-circuited and the depolarisation current, I, was measured during the heating from −30 °C to 150 °C at 10 °C/min to obtain a complex spectrum.

3. Results

DSC analysis was performed between the glass transition and the fusion of the two series of samples. The DSC observations of the cold crystallisation and of the fusion are as expected and are documented in the literature for PET [27–29] and PLLA [30,31]. Thus, they are not shown here and we focused on the amorphous phases as shown in Figs. 2 and 3 displaying glass transition of PET and PLLA annealed samples. To quantify the different phases inside the samples, the crystallinity induced by the thermal treatment at T_a must be calculated first. This degree of crystallinity X_c could be deduced from the heating DSC data using the following equation:

$$X_c = \frac{\Delta H_f - \Delta H_c}{\Delta H_f^0} \quad (1)$$

in which ΔH_f is the measured enthalpy of fusion, ΔH_f^0 is the calculated enthalpy of fusion of a wholly crystalline material ($\Delta H_f = 140$ J/g for PET [32] and $\Delta H_f = 93$ J/g for PLLA [33]) and ΔH_c is the cold crystallisation enthalpy obtained during the DSC runs. Indeed, the experimental enthalpy of fusion ΔH_f corresponds to the fusion of the whole crystal part of samples, i.e. the crystalline phase already present before the DSC scan and the crystalline phase developed during the scan which is measurable by the peak of cold crystallisation. The variations of X_c vs. t_a reported in Fig. 4 show a quasi-sigmoidal increase of X_c. For PET, a wholly amorphous sample could not be obtained and the minimum X_c calculated from Eq. (1) was close to 7%. Schmidt-Rohr et al. [34] also tried to prepare a completely amorphous PET but they always found a residual crystallinity of 5%. For every cold crystallisation time $t_a \leq 40$ min, X_c remains constant. For t_a included between 40 min and 350 min, a crystalline phase consisting of spherulites appears in the sample. Optical micrographs of similar cold-crystallised PLLA can be found elsewhere [35,36]. For longer times, the degree of crystallinity remains constant and is close to 27%. For PLLA, contrary to the PET, our procedure allowed to obtain a fully amorphous sample (it has been confirmed by X-ray diffraction analysis). The degree of crystallinity remains null till a time t_a of 10 min. Then, X_c sharply increases from 20 min to 60 min to reach a value around 43%. This value which is the maximum degree obtained is higher than the PET value. It could be attributed to the difference between the constitutive units. PLLA ones do not contain aromatic rings and macromolecule rearrangements are probably easier. We now focus on the glass transition in Figs. 2 and 3. For the non-treated PET sample ($t_a = 0$ min) the heat flow step is sharp (≈15 °C) and has a value corresponding to 0.30 J/g K. The small overshot at the glass transition is linked to fast relaxation processes inside the material. For the first four t_a, the heat flow steps have the same value. When increasing t_a up to 300 min, the shape of this step remains the same but the heat flow step at T_g decreases with t_a increasing. For $t_a \geq 350$ min, the shape of the curve changes and the temperature zone of the phenomenon widens. For these samples, the degree of crystallinity is maximum. A similar evolution can be observed for PLLA: under $t_a \leq 70$ min, the shape remains the same and only the heat flow step decreases, while for $t_a \geq 80$ min the shape changes and temperature zone of T_g is enlarged. The same overshot as for PET is observable for low X_c. It is interesting to report the range in which the

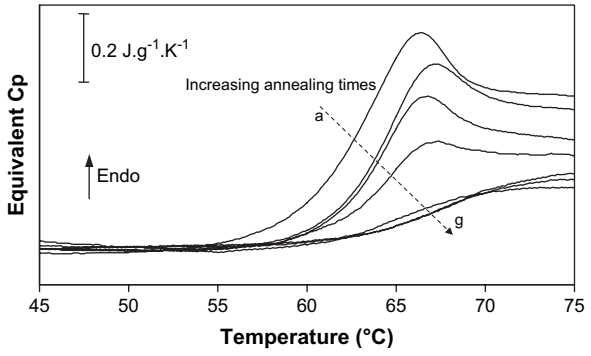

Fig. 3. DSC curves around the glass transition of a PLLA cold-crystallised at 80 °C for different durations (from a to g: 0, 30, 40, 50, 70, 120 and 150 min). Equivalent Cp is the heat flow normalised to the mass and to the heating ramp.

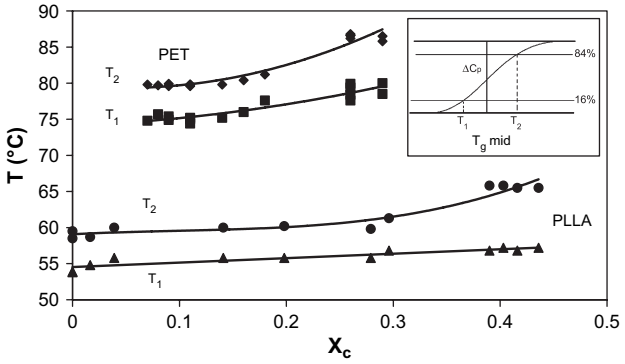

Fig. 5. Variations of T_1 and T_2 calculated from Donth's model plotted against the degree of crystallinity for PET (on top) and PLLA.

glass transition occurs as a function of the crystallisation degree. It allows to have an overview on the influence of the crystalline phase on the remaining amorphous phase. Consequently, we propose to use Donth's procedure [37] by measuring two temperatures T_1 and T_2, respectively, corresponding to 16% and 84% of the heat capacity step. These two temperatures are plotted as a function of the degree of crystallinity as shown in Fig. 5. By having a look on PET, from $X_c = 7\%$ to 14%, T_1 and T_2 remain constant. Beyond these X_c, T_1 increases by 5 °C while T_2 increases by 7 °C. This trend is due to the influence of the crystalline phase, which probably constrains and rigidifies the amorphous phase. Moreover, the widening of $\Delta T = T_2 - T_1$ (around 2 °C) is significant of a larger amorphous phase heterogeneity.

Concerning PLLA, T_1 and T_2 increase very slowly up to 30% of crystallinity (corresponding to 60 min at 80 °C cold crystallisation time). For the longest crystallisation times (achievement of the maximum degree of crystallinity), T_1 keeps on increasing slowly (+2 °C), while T_2 raises 7 °C up. As described for PET, the crystalline phase only influences the amorphous one at high crystallinity degrees, while for PET this influence already appears from $X_c = 15\%$. For PET, T_1 and T_2 increase more than 5 °C, so we can suppose that the molecular mobility decreases in the whole amorphous phase. For PLLA, the increase in T_1 is weaker than in T_2. So, a small part of the amorphous phase is modified by the crystalline phase but the main part of this amorphous phase does not seem to undergo any influence from the crystalline phase. Note that in other PLLA systems, by using other kinds of DSC and dielectric spectroscopy experiments, it was possible to detect a more gradual change in the glass behaviour, where the existence of two independent (inter- and intra-spherulitic) mobile amorphous phases was suggested [35,38].

In the following, we propose to compare four materials:

- A weakly crystallised PET ($X_c = 8\%$) and a non-crystallised PLLA ($X_c = 0\%$).
- Two cold-crystallised samples in which the maxima of crystallinity have been obtained: one is a PET corresponding to a crystallisation time of 720 min ($X_c = 29\%$) and the second is a PLLA with a crystallisation time of 120 min ($X_c = 40\%$).

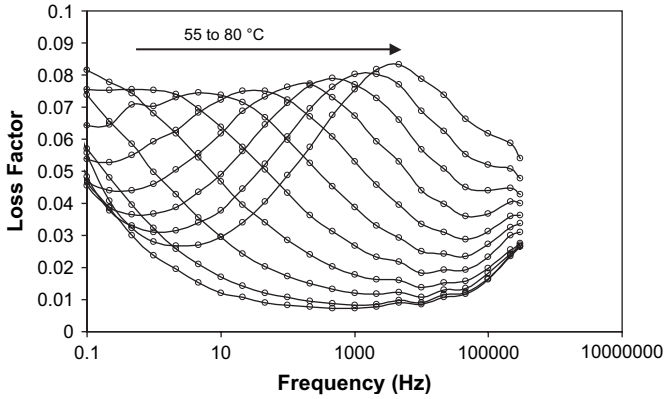

Fig. 6. Example of a DS analysis obtained on PLLA: loss factor (ε'') as a function of the frequency for temperature ranging from 55 °C to 80 °C by steps of 2.5 °C.

Fig. 6 shows, as an example, the dielectric loss factor (ε'') depending on the frequency for different temperatures. This curve is that of the semi-crystalline PLLA and for the other samples, the same kind of analysis was obtained. A relaxation peak is observed. This peak is the dielectric manifestation of the glass transition of the PLLA amorphous phase and will be labelled α mode as the main relaxation mode. A classical behaviour is observed: the dielectric loss peak shifts to higher frequencies with increasing temperatures. This temperature dependence is characteristic from the amorphous phase molecular mobility above T_g.

As shown in Fig. 7, the TSDC manifestation of the glass transition is evidenced by a depolarisation current peak called α peak which exhibits a maximum at the temperatures $T_\alpha = 74$ °C and 59 °C for the non-crystallised PET and PLLA, respectively. For TSDC the depolarisation current peak results from cooperative motions of dipoles, while for DSC a heat flow step related to cooperative conformational rearrangements of segments of the macromolecular chains is observed. These two techniques give responses due to the glass transition appearing in the same temperature range. For the two semi-crystalline samples, an increase of the temperature of the maximum T_α and a decrease in the peak magnitude are observed,

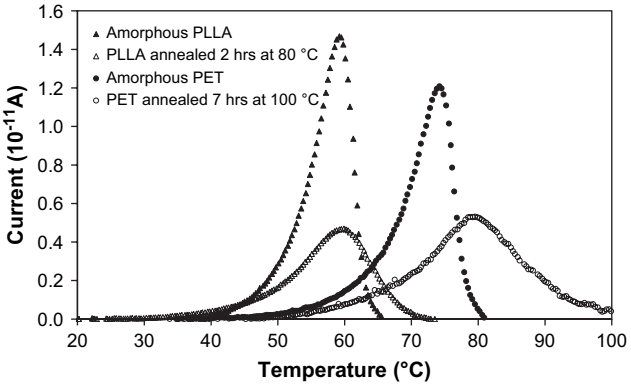

Fig. 7. Experimental TSDC curves of amorphous PET and PLLA (black circles and triangles, respectively), cold-crystallised PET at 100 °C for 720 min (empty circles) and cold-crystallised PLLA at 80 °C for 120 min (empty triangles).

while the shape of the peak becomes wider (indicative of more heterogeneity). The increase of T_α is +5 °C and only +1 °C for the crystallised PET and PLLA, respectively. As for DSC, the variations are more important in PET than in PLLA. So, the whole amorphous phase of PET seems to be modified: the rigidity and the heterogeneity increases, while in PLLA the heterogeneity increases too but not quite as much as in PET.

4. Discussion

4.1. Three-phase model

Typically, it is possible to calculate the fraction of amorphous phase X_{am} from the ΔC_p step data at the glass transition:

$$X_{am} = \frac{\Delta C_p}{\Delta C_{p0}} \quad (2)$$

where ΔC_p is the thermal heat capacity step at T_g of an annealed sample and ΔC_{p0} that of a 100% amorphous sample. The choice of this value is obviously of great importance in the following. Concerning PET, the ATHAS database [32] suggests a heat capacity increment of 0.405 J/g K. This value is in agreement with our previous results. For PLLA, as our quenched samples controlled by DSC and X-ray diffraction are wholly amorphous, ΔC_{p0} was carefully measured and a value of 0.48 J/g K can be proposed.

In the case of PET, the decrease of X_{am} is very important when X_c increases (Fig. 8) and the data are not along the line of equation $X_c + X_{am} = 1$. As a consequence, a part of the amorphous phase does not participate to the glass transition. This rigid amorphous fraction RAF must be taken into account as the third element of a three-phase model such as $X_{am} + X_c + X_{ar} = 1$ where X_{ar} describes the contribution of the RAF. For PLLA, the couples of data are really close to the line of equation $X_c + X_{am} = 1$ up to a crystallisation time of 70 min (achievement of the maximum crystallinity inside the sample): the two-phase model is relevant to describe the material. But, as soon as the maximum X_c is achieved, the crystallisation treatment influences the amorphous phase: even if crystallites cannot be created anymore, the thermal treatment acts on the amorphous phase by transforming a part of the mobile amorphous phase into a rigid amorphous one.

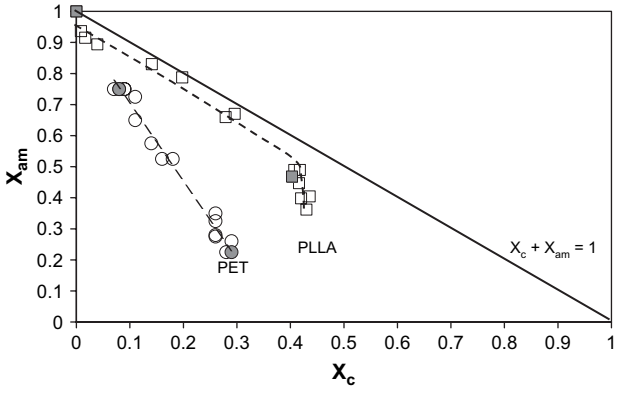

Fig. 8. PET (empty circles) and PLLA (empty squares) mobile amorphous fractions as a function of the degree of crystallinity. The $X_{am} + X_c = 1$ line corresponds to the theoretical two-phase model. The grey points represent samples focused on in this paper.

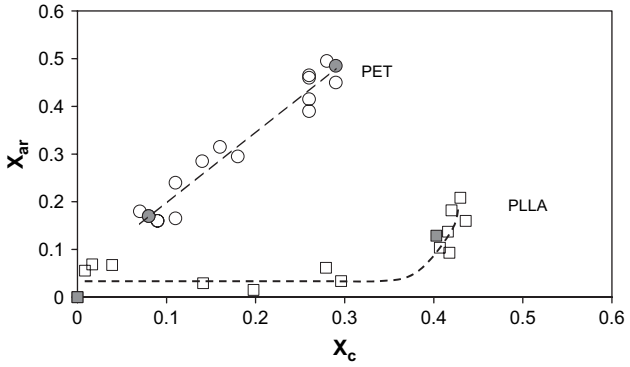

Fig. 9. Degree of crystallinity dependence of the rigid amorphous fraction for PET (empty circles) and for PLLA (empty squares). The grey points represent samples focused on in this paper.

Fig. 9 displays the variation of the rigid amorphous fraction ($X_{ar} = 1 - X_{am} - X_c$) as a function of the crystallinity degree (X_c). In PET, X_{ar} quasi-linearly increases and reaches 50% of the material, while for PLLA, X_{ar} remains very weak up to $X_c = 40\%$ but drastically increases up to 25% of the material as the crystallisation time increases.

From these three last curves (Figs. 7–9), the microstructure of a semi-crystalline PET is well described by the three-phase model. For very low X_c, X_{ar} is also low (less than 20%) and the remaining amorphous phase does not seem to undergo any influence from the crystallites. But as X_c grows, X_{ar} linearly increases too, confirming the idea that the rigid amorphous fraction surrounds the crystallites lamellae. As soon as the maximum X_c is reached, and as the annealing continues, the three-phase model is still relevant as the remaining mobile amorphous phase becomes rigid and more heterogeneous.

Contrary to the PET, PLLA can practically be described by a two-phase model until achieving the maximum of crystallinity. This behaviour could be explained by a better chain flexibility as the PLLA constitutive monomer does not contain any aromatic cycle (Fig. 1). The decoupling between the crystalline and the amorphous phase is better than that in PET. Nevertheless, for the longest crystallisation durations, a part of the amorphous phase becomes rigid (but it only reaches half of the PET X_{ar}). The PLLA then obeys the three-phase model with a modified mobile amorphous phase (the characteristic temperatures are shifted to higher temperatures). It could be attributed to a diminution of the free volume in the amorphous phase induced by the annealing. Following Androsch and Wunderlich [6], the specific RAF, i.e. the ratio between the rigid amorphous fraction and the crystalline phase degree, was calculated (see Table 1). The specific RAF can be considered as the average amount of rigid amorphous structure per unit of crystal. In the case of the PET, the specific RAF is large and decreases from 2.1 to 1.7 for a crystallinity degree from

Table 1
Parameters of the four studied samples

	X_c	X_{am}	X_{ar}	Specific RAF $= X_{ar}/X_c$	$\tau(T_g)$ (s)	m	m_g
a-PET	0.08	0.75	0.17	2.1	6	133	120
sc-PET	0.29	0.22	0.49	1.7	90	65	33
a-PLLA	0	1	0	–	2	189	118
sc-PLLA	0.40	0.47	0.13	0.3	9	173	65

0% to 29%. Our values are consistent with Androsch's results: for a cold-crystallised PET with $X_c = 24\%$, values included between 5 and 1.7 are given. After additional annealing, the specific RAF continues to decrease down to 0.75, indicating an increase of decoupling between crystalline and amorphous phases. For the samples studied in this work, the decrease was less significant but not in contradiction. During crystallisation, the crystalline phase essentially grows to the detriment of the amorphous phase. For PLLA, the specific RAF is weak (0.3) which means an important decoupling of the crystalline and the amorphous phase. Due to the absence of aromatic cycle, the PLLA macromolecule is more flexible than PET, and the folding of the molecule on the crystal surface is probably more important. So, there exist less tie molecules between crystal and amorphous phases in PLLA than in PET.

It is now interesting to characterise the mobile amorphous phase in terms of relaxation time and fragility. We focus on the four samples studied by DSC and TSDC: two samples with the minimum degree of crystallinity (and called a-PET and a-PLLA) and two semi-crystalline samples called sc-PET and sc-PLLA. The corresponding values of X_c, X_{am} and X_{ar} are reported in Table 1.

4.2. Parameters of the mobile amorphous phase

From the DS peaks characterising the α relaxation (dielectric manifestation of the glass transition), relaxation time τ can be obtained. This time was calculated by taking the frequency at the maximum of the peak for each isothermal curve ($\tau = 1/2\pi f$). The variations of log τ vs. 1000/T were plotted (Fig. 10) for each sample. They are very similar for a-PLLA and sc-PLLA, only a small shift in temperature can be observed. For the a-PET and the two PLLA samples, variations of log τ vs. 1000/T are not linear and can be fitted by the Vogel–Tamman–Fulsher relationship [12–14]. For the sc-PET, the variations are very different from those of the a-PET, as the variations are quasi-linear and follow the Arrhenius law. Thus, as previously observed on strain induced crystallised PET samples [22], variations of the relaxation time obtained by dielectric spectroscopy showed that amorphous PET can be classified as "fragile", while semi-crystalline PET exhibits a "strong" behaviour. For PLLA, the amorphous phase remains "fragile" even if a crystalline phase is present inside the sample.

Variations of the relaxation time τ with the temperature can also be obtained from TSDC data. Indeed, the relaxation time

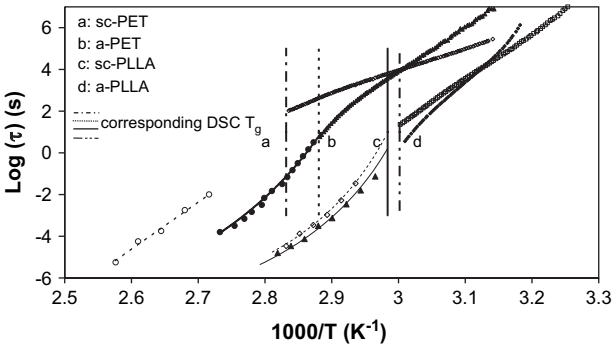

Fig. 10. Relaxation times calculated as a function of the temperature for the four samples obtained thanks to DS and TSDC measurements. (a) Cold-crystallised PET (sc-PET), (b) non-treated PET (a-PET), (c) cold-crystallised PLLA (sc-PLLA) and (d) non-treated PLLA (a-PLLA). The vertical lines correspond to the T_g mid-point measured in DSC for each sample.

$\tau(T)$ of the glass transition dielectric manifestation can be calculated by different formalisms. Alegria et al. have shown that the α relaxation must be analysed with the Kohlrausch–Williams–Watts (KWW) equation [39] and τ can be written as

$$\tau = \beta \frac{Q}{I}\left[\ln \frac{Q_0}{Q}\right]^{[1-1/\beta]} \tag{3}$$

where $Q(t) = \int_t^\infty I\, \mathrm{d}t$, Q_0 being the value of the initially stored charge, and β is a parameter accounting for the non-Debye character of the α relaxation. As pointed out before, DSC results show a broadening of the glass transition for the highest degree of crystallinity. This can be due to different reasons [18]: (i) a decrease in the apparent activation energy around T_g; (ii) an increase of the composition heterogeneity (link to the presence of RAF); (iii) an intrinsic broadening of the relaxation time distribution. If the latter hypothesis is one of the causes of the broadening, variation of the KWW parameter β values could be expected. For a-PET and sc-PET, it has been shown that β is 0.41 and 0.34, respectively [18,20] while for a-PLLA and sc-PLLA, similar β values were proposed before (0.41 and 0.35, respectively [23]).

The TSDC variations of log τ vs. 1000/T are also reported in Fig. 10. For PET, data are well separated between the amorphous and the semi-crystalline samples: if the sc-PET presents a quasi-linear variation, a curvature for amorphous PET is observable at temperatures close to T_g. For the PLLA materials, the data are closer to each other. The vertical lines reported in the figure correspond to the DSC values of the glass transition temperature (the abscises are 1000/T_g with T_g the mid-point temperature). It can be observed that the temperature domains for which the data are collected with DS and TSDC are complementary. Thus, it is clear that the TSDC data concern relaxation phenomena occurring in the glassy state [40], while DS data concern relaxation phenomena occurring in the liquid-like state. Finally, it can be said that the profile of the relaxation time variations presented in Fig. 10 is typical of the glass transition region and has also been observed by means of creep and dynamic mechanical analysis [41]. The ensemble of results for each material, except sc-PET due to its "strong"

character, then suggests a change from a Vogel–Tamman–Fulsher behaviour, in the thermodynamic equilibrium state, towards an Arrhenius regime, in the glassy state. Such behaviour was also found in sc-PLLA from dynamic mechanical analysis measurements [42], and could be ascribed to the progressive freezing of configurational entropy when a glass-forming system enters through the glassy state upon cooling. All data series fitted with the ad hoc formula intersected each others at a temperature very close to the DSC T_g and at a relaxation time around 10 s (values reported in Table 1). The calculation of the fragility index m can be done from TSDC and SD techniques according to [22] and using the following equation:

$$m = \frac{\mathrm{d}(\log(\tau))}{\mathrm{d}(T_g/T)_{T=T_g}} \tag{4}$$

In the following, the DSC mid-point T_g value has been chosen to calculate the fragility indexes from DS and TSDC data. It has been previously shown that the TSDC fragility index is the one characterising the glassy state (m_g as defined by Hutchinson [43]) and the DS fragility index is the one characterising the glass-forming liquid (m). For the a-PLLA and the a-PET, the fragility indexes m are 189 and 133, confirming these materials must be classified as ''fragile'' glass-forming liquids. For sc-PET (with only 22% of mobile amorphous phase), the fragility is significantly lower ($m = 65$) than for a-PET. The behaviour of the semi-crystalline material goes towards a ''strong character'' which is consistent with the quasi-Arrhenius variations of log (τ). An important decrease of m_g is observable from a-PET to sc-PET. So, due to the weak percentage of mobile amorphous phase and to the chemical structure, the relaxation phenomena in the glassy and the liquid states are completely different from those of a quasi-amorphous material.

For the sc-PLLA (in which the mobile amorphous phase represents 47% of the material), there exists no significant change of m ($m = 173$ for sc-PLLA, 8% less than for a-PLLA and with an uncertainty equal to 10%). So, the presence of the crystalline phase and of a rigid amorphous fraction does not significantly modify PLLA fragility parameters, i.e. the variations of the relaxation times with the temperature when the temperature approaches the glass transition. The fragility indexes of the glassy states m_g show a significant variation: a decrease from a-PLLA to sc-PLLA. This decrease (from 118 to 65) is half that observed for PET (from 120 to 33). This difference between m and m_g variations is of interest and further investigations will have to be done to confirm it. As previously shown, modifications appear in the PLLA mobile amorphous phase when the crystalline phase is present: on one hand, the shape of the TSDC α-peak is modified, the characteristic temperature of the end of the DSC glass transition (T_2) increases. This indicates a higher heterogeneity and a significant modification of the rigidity for a part of the amorphous phase (probably the part of the mobile amorphous phase close to the rigid amorphous fraction). On the other hand, the TSDC T_α and the T_1 DSC temperatures vary very slowly contrary to the PET temperatures. So, a part of the mobile amorphous phase remains practically the same even if a crystalline phase is present, and only the fragility parameter characteristic of the glassy state changes. This result is very interesting and a first hypothesis can be proposed here following Wunderlich's approach [5]: above the glass transition, the RAF progressively disappears and the material returns to a two-phase model. So, in the case of PET, the RAF percentage is high enough to be ''detected'' and influences the fragility indexes values above and below T_g. In the case of PLLA, the low percentage of RAF is enough to modify fragility index below T_g, but above T_g, this RAF quickly disappears, the amorphous phase fragility being practically independent of the degree of crystallinity.

5. Conclusion

Amorphous PET and PLLA can be classified as ''fragile'' material like many other polymers. The variations of the characteristic relaxation time in the liquid-like state are important. When a cold crystallisation is performed in PET, the material must be described as a three-phase material: the crystalline phase, the amorphous phase and an additional fraction consisting of tie molecules between the amorphous and the crystalline phases. This rigid amorphous fraction represents the main part of the material in the fully crystallised PET (49%, see Table 1). This study has clearly shown that there exists a strong coupling between the RAF and the remaining amorphous phase. All the parameters of the amorphous phase studied are different between the amorphous and the semi-crystalline PET. The latter goes from a ''fragile'' to a ''strong'' character as soon as it becomes semi-crystalline. So, the confinement of the a-phase by the RAF has modified the glass transition dynamic.

Concerning PLLA, the appearance of a crystalline phase has a lower influence as only few parameters vary. In sc-PLLA, the RAF is lower (13% for highly crystallised PLLA) and the coupling between the crystals and the amorphous phase is weaker than in PET. We attributed this difference to more flexible macromolecules in PLLA. The coupling between the RAF and the mobile amorphous phase is also weak. The glass transition dynamic is only slightly modified and the material remains ''fragile''. Nevertheless, some parameters of the amorphous phase have changed showing there is some coupling. This work has pointed out to an important and new result concerning PLLA fragility. When the degree of crystallinity increases, the fragility index m of the glass former liquid remains constant while the fragility index of the glassy state varies. It is attributed to a rapid disappearance of the RAF above the glass transition, and as a consequence, of the coupling between the phases.

References

[1] Auras RA, Harte B, Selke S, Hernandez R. J Plast Film Sheet 2003;19:123.
[2] Suzuki H, Grebowicz J, Wunderlich B. Br Polym J 1985;17:1.
[3] Menczel J, Wunderlich B. J Polym Sci Polym Lett 1981;1:261.
[4] Kattan M, Dargent E, Grenet J. Polymer 2002;43:1399.

[5] Wunderlich B. Prog Polym Sci 2003;28:383.
[6] Androsch R, Wunderlich B. Polymer 2005;46:12556.
[7] Angell CA. In: Ngai KL, Wright GB, editors. Relaxation in complex systems. Washington: Naval Research Laboratory; 1984. p. 3.
[8] Plazek DJ, Ngai KL. Macromolecules 1991;24:1222.
[9] Bureau E, Chebli K, Cabot C, Saiter JM, Dreux F, Marais S, et al. Eur Polym J 2001;37:2169.
[10] Godard ME, Saiter JM. J Non-Cryst Solids 1998;235:635.
[11] Saiter A, Hess M, D'Souza NA, Saiter JM. Polymer 2002;43:7497.
[12] Vogel H. Phys Z 1921;22:645.
[13] Fulcher GS. J Am Ceram Soc 1925;8:339.
[14] Tammann G, Hesse G. Z Anorg Allg Chem 1926;156:245.
[15] Montserrat S, Cortés P. J Mater Sci 1995;30:1790.
[16] Dobbertin J, Hensel A, Schick C. J Therm Anal 1996;47:1027.
[17] Zhao J, Song R, Zhang Z, Linghu X, Zheng Z, Fan Q. Macromolecules 2001;34:343.
[18] Alves NM, Mano JF, Balaguer E, Meseguer Dueñas JM, Gómez Ribelles JL. Polymer 2002;43:4111.
[19] Ezquerra TA, Baltà-Calleja FJ, Zachmann HG. Polymer 1994;35:2600.
[20] Fukao K, Miyamoto Y. J Non-Cryst Solids 1997;212:208.
[21] Alvarez C, Šics I, Nogales A, Denchev Z, Funari SS, Ezquerra TA. Polymer 2004;45:3953.
[22] Dargent E, Bureau E, Delbreilh L, Zumailan A, Saiter JM. Polymer 2005;46:3090.
[23] Mano JF, Gómez Ribelles JL, Alves NM, Salmerón Sanchez M. Polymer 2005;46:8258.
[24] Hu Y, Rogunova M, Topolkaraev V, Hiltner A, Baer E. Polymer 2003;44:5701.
[25] Van Turnhout J. Thermally stimulated discharge of polymer electrets. Amsterdam: Elsevier; 1975.
[26] Dargent E, Santais JJ, Saiter JM, Bayard J, Grenet J. J Non-Cryst Solids 1994;172:1062.
[27] Minakov AA, Mordvintsev DA, Schick C. Polymer 2004;45:3755.
[28] Kong Y, Hay JN. Polymer 2003;44:623.
[29] Goschel U. In: Fakirov S, editor. Handbook of thermoplastic polyesters. Weinheim: Wiley-VCH; 2002. p. 291.
[30] Di Lorenzo ML. Polymer 2001;42:9441.
[31] Tsujo H, Ikada Y. Polymer 1995;36:2709.
[32] ATHAS Data Bank, http://web.utk.edu/~athas/databank/.
[33] Fischer EW, Sterzel HJ, Wegner G. Kolloid Z Z Polym 1973;251:980.
[34] Schmidt-Rohr K, Hu W, Zumbulyadis N. Science 1998;280:714.
[35] Wang Y, Gómez Ribelles JL, Salmerón Sánchez M, Mano JF. Macromolecules 2005;38:4712.
[36] Wang Y, Funari SS, Mano JF. Macromol Chem Phys 2006;207:1262.
[37] Donth E, Korus J, Hempel E, Beiner M. Thermochim Acta 1997;304:239.
[38] Dionísio M, Viciosa MT, Wang Y, Mano JF. Macromol Rapid Commun 2005;26:1423.
[39] Alegria A, Goitiandia L, Colmenero J. J Polym Sci Part B Polym Phys 2000;38:2105.
[40] Saiter JM, Dargent E, Kattan M, Cabot C, Grenet J. Polymer 2003;44:3995.
[41] Alves NM, Mano JF, Gomez Ribelles JL, Gomez Tejedor JA. Polymer 2004;45:1007.
[42] Mano JF. Macromol Biosci 2005;5:337.
[43] Hutchinson JM. Polym Int 1998;47:56.